Biophysical Journal, Volume 96

Supporting Material

Effect of voltage sensitive fluorescent proteins on neuronal excitability

Walther Akemann, Alicia Lundby, Hiroki Mutoh, and Thomas Knöpfel

Effect of voltage sensitive fluorescent proteins on neuronal excitability

Walther Akemann[1], Alicia Lundby[1,2], Hiroki Mutoh[1] and Thomas Knöpfel[1]

[1]Laboratory for Neuronal Circuit Dynamics, RIKEN Brain Science Institute,
2-1 Hirosawa, Wako-City, Saitama 351-0198, JAPAN

[2]The Danish National Research Foundation, Centre for Cardiac Arrhythmia,
University of Copenhagen, 2200 Copenhagen, DENMARK

Supplementary Material

Supplement 1:
VSFP-imaging at the shot noise limit

The following paragraph summarizes assumptions and formulas that we used to estimate the VSFP signal-to-noise relation for spike detection in single neurons.

The imaged neuron is approximated by a membrane sphere of fixed diameter, which is supposed to represent the somatic and perisomatic membrane of a large rodent relay neuron. As a consequence of photonic shot noise, the total number of detected photons n_T per sampling time interval fluctuates stochastically around a mean value $<n_T>$ according to the Poisson distribution. For larger numbers of emitters the photon distribution approaches a normal Gauss distribution (central limit theorem) with a standard deviation of $\sqrt{<n_T>}$:

(S1.1) $$\frac{1}{\sqrt{< n_T >}} \cdot \varphi_N \left(\frac{n_T - < n_T >}{\sqrt{< n_T >}} \right)$$

with φ_N the standard normal distribution. The total number of detected photons n_T is made up of n_S signal photons and n_B photons of background fluorescence originating from non-responsive VSFP and tissue auto-fluorescence. The actual response signal is carried by a number of Δn_S photons riding on a baseline signal of n_{S0} photons with $|\Delta n_S| << n_{S0}$:

(S1.2) $$n_T = n_B + n_S = n_B + n_{S0} + \Delta n_S$$

From Eqs. (S1.1 and S1.2) it follows that the total photon signal including shot noise obeys to the following relation:

(S1.3) $$n_T = \frac{1}{1 - f_B} \cdot < n_S > + \frac{1}{\sqrt{1 - f_B}} \cdot \sqrt{< n_S >} \cdot r_N$$

where f_B is the fraction of non-responsive background $f_B := <n_B> / <n_T>$ and r_N is a random number drawn from a standard normal distribution.

The average number of detected photons in a given measurements will depend on the total number of contributing VSFP emitters, the yield for VSFP fluorescence, the efficiency of the detection optics and the bandpass and intensity of fluorescence excitation:

(S1.4) $$< n_{S0} >= f_C \cdot f_{em} \cdot q_D \cdot < I_{em} > \cdot \Delta t$$

where f_C denotes the fraction of emission light collected by the objective, f_{em} the fraction of the emission spectrum transmitted to the detector, q_D the detector quantum yield, I_{em} the total emission rate under baseline conditions and Δt the sampling interval. As the molecular emission, under common experimental conditions, is limited by photo-bleaching rather than excited state saturation, the emission rate I_{em} is practically determined by the amount of photobleaching deemed acceptable in a given measurement by adjustment of excitation intensity. With assumed mono-exponential photobleaching this gives:

(S1.5) $$< I_{em} >= n_F \cdot q_{em} \cdot \sigma_{abs} \cdot I_{ex} \approx n_F \cdot \frac{q_{em}}{q_{pb} \cdot \tau_{pb}}$$

with n_F the total number of VSFP units contributing to the emission signal, σ_{abs} the molecular cross section for photo absorption at the wavelength of excitation, I_{ex} the intensity of excitation light, q_{em} the quantum yield of fluorescence, q_{pb} the quantum yield of photobleaching and τ_{pb} the photobleaching time constant. Finally, the wanted signal S and signal to noise ratio, $R_{S/N}$, are given as:

$$< S >= \left| < \Delta n_S > \right| = \left| \frac{\Delta F}{F_0} \right| \cdot < n_{S0} >$$

(S1.6)

$$R_{S/N} = \frac{< S >}{\sqrt{< n_T >}} = \left| \frac{\Delta F}{F_0} \right| \cdot \sqrt{1 - f_B} \cdot \sqrt{< n_{S0} >}$$

with $\Delta F/F_0$ the normalized VSFP quantum response. Combining equations (S1.2, S1.4-1.6) results in the following expression for the expected S/N in a VSFP recording from a neuron with a spherical membrane of diameter D and a VSFP membrane density ρ:

(S1.7)
$$R_{S/N} = \left| \frac{\Delta F}{F_0} \right| \cdot \sqrt{1 - f_B} \cdot \sqrt{\rho \cdot \pi \cdot D^2} \cdot \sqrt{f_C \cdot f_{em} \cdot q_D} \cdot \sqrt{\frac{q_{em} \cdot \Delta t}{q_{pb} \cdot \tau_{pb}}}$$

As a result of noise the event detection will produce false positive events (falsely detected spurious events) with a probability depending on the discrimination method and the $R_{S/N}$ of the data. For the same reason the method will fail to detect true events with a certain true-negative probability. If positive events are identified by a signal threshold $S_{threshold}$ the false-positive, p_{FP}, and true-negative, p_{TN}, probabilities are calculated from the photon distribution (Eq. S1.1) as:

$$p_{FP}(x_{threshold}) = \frac{1}{2} \cdot \left[1 - erf\left(\frac{x_{threshold}}{\sqrt{2}} \right) \right]$$

(S1.8)

$$p_{TN}(x_{threshold}) = \frac{1}{2} \cdot \left[1 + erf\left(\frac{x_{threshold} - R_{S/N}}{\sqrt{2}} \right) \right]$$

with $x_{threshold} := S_{threshold} / <N>$ the detection threshold normalized by <N>: $=\sqrt{<n_T>}$ the mean noise amplitude. The two probabilities become equal at $x_{threshold} = R_{S/N}/2$, equivalent to a signal threshold of half of the mean signal amplitude, thus:

(S1.9)
$$p_{FP} = p_{TN} = \frac{1}{2} \cdot \left[1 - erf\left(\frac{1}{2\sqrt{2}} \cdot R_{S/N} \right) \right]$$

As long as the detection probability is not limited by the sampling, the true-positive probability, p_{TP}, for the positive detection of a true event follows as $p_{TP} = 1 - p_{TN}$.

Supplement 2
VSFP single-barrier model

If the movement of the VSD (voltage sensing domain) charge is rate-determined by a single transition, then the activation and deactivation of the sensor are described as a Hodgkin-Huxley mechanism with a single state variable ($0 \le n_{VSFP} \le 1$) obeying a first-order rate equation (analogous to Eq. 1) with the ON/OFF rate coefficients given by:

$$S_{ON}(V) = \left(\frac{1}{2\tau_{1/2}}\right) \cdot \exp\left(\frac{z \cdot e_0 \cdot \delta}{k_B T} \cdot \left(V - V_{1/2}\right)\right)$$
$$S_{OFF}(V) = \left(\frac{1}{2\tau_{1/2}}\right) \cdot \exp\left(-\frac{z \cdot e_0 \cdot (1-\delta)}{k_B T} \cdot \left(V - V_{1/2}\right)\right) \quad \text{(S2.1)}$$

with $\tau_{1/2}$, the time constant at half activation, z, the valence of sensing charge, e_0, the elementary charge, δ, the ON/OFF asymmetry ($0 \le \delta \le 1$), k_B, the Boltzmann constant, T the absolute temperature and $V_{1/2}$, the voltage of half activation. The charge movements give rise to a sensing capacitance C_{VSFP} of cell membranes expressing VSFP protein:

$$C_{VSFP} := I_{VSFP} \cdot \left(\frac{dV}{dt}\right)^{-1} = \rho \cdot z \cdot e_0 \cdot \frac{dn_{VSFP}}{dV} \quad \text{(S2.2)}$$

with I_{VSFP}, the sensing current density and ρ, the number of VSFP units per unit area. The value of n_{VSFP} in steady state follows from Eq. S2.1 as:

$$n_{VSFP}^{\infty} = \frac{S_{ON}}{S_{ON} + S_{OFF}} = \left[1 + \exp\left(-\frac{z e_0}{k_B T} \cdot \left(V - V_{1/2}\right)\right)\right]^{-1} \quad \text{(S2.3)}$$

Combining equations S2.2 and S2.3 gives the sensing capacitance in quasi-steady state:

$$C_{VSFP}^{\infty}(V) = \rho \cdot \frac{(z e_0)^2}{k_B T} \cdot n_{VSFP}^{\infty}(V) \cdot \left[1 - n_{VSFP}^{\infty}(V)\right] \quad \text{(S2.4)}$$

Under quasi-steady state conditions the fluorescence signal follows the activation of the sensor according to:

$$F^{\infty} = F_{1/2} + \Delta F_{\max} \cdot \left(n_{VSFP}^{\infty} - \frac{1}{2}\right) \quad \text{(S2.5)}$$

where $F_{½}$ denotes the fluorescence signal at half activation and ΔF_{max} the maximum fluorescence modulation corresponding to the difference of the steady-state fluorescence at large depolarizing and large hyperpolarizing potentials. ΔF_{max} divided by $F_{1/2}$ is a measure of the dynamic range of the fluorescence modulation of the protein. Using Eq. S2.3 and S2.5 the voltage sensitivity, $S_{½}$, of the sensor at half activation follows as:

$$S_{1/2} := \left(F_{1/2}\right)^{-1} \cdot \left(\frac{dF^{\infty}}{dV}\right)_{1/2} = \frac{1}{4} \cdot \frac{\Delta F_{\max}}{F_{1/2}} \cdot \frac{z e_0}{k_B T} \quad \text{(S2.6)}$$

Hence, $S_{½}$ increases linearly as function of the gating charge and dynamic range of fluorescence.

Supplement 3:
Signal discrimination and S/N in neuron voltage imaging using VSFPs

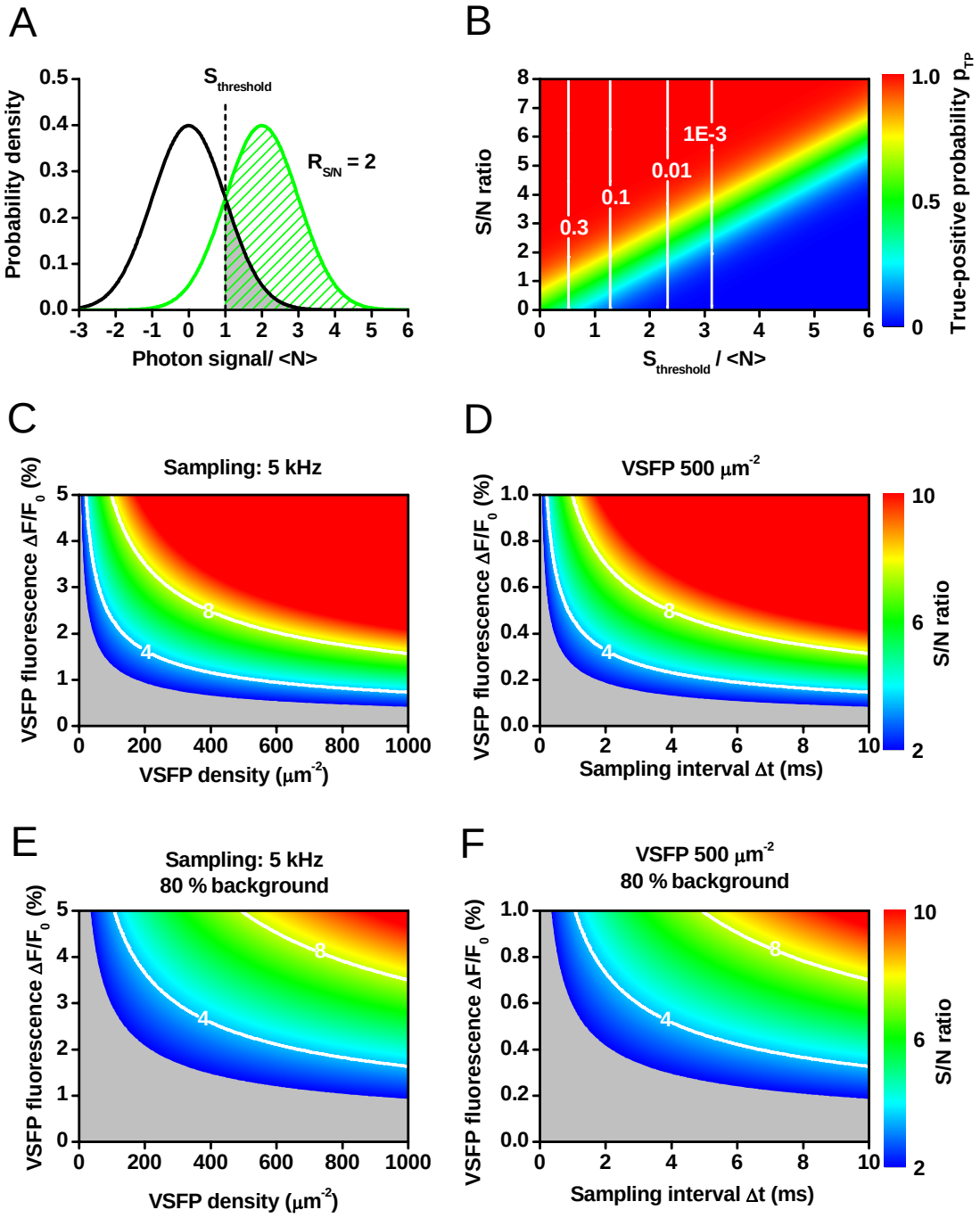

Fig. S1: Signal discrimination and S/N in VSFP neuron voltage imaging evaluated from the equations given in Supplement 1.
(A) Photon distribution of the VSFP baseline signal F_0 - $\langle F_0 \rangle$ (black color) and the response signal F - $\langle F_0 \rangle$ (green color) for the case of S/N of 2. The signal amplitude is given in units

of <N>, the mean amplitude of photon noise. The signal threshold $S_{threshold}$ (dotted line) is set to <ΔF>/2, half of the mean signal amplitude. Hatched (shaded) areas indicate true-positive (false-positive) detection probabilities. **(B)** True-positive probability p_{TP} for successful detection of a signal event as function of detection threshold $S_{threshold}$ (in units of <N>, the mean noise amplitude) and signal-to-noise ratio $R_{S/N}$ according to Eq. S1.8. Probabilities are color-coded according to the scale given to the right. White contour lines indicate probabilities for false-positive events. **(C)** S/N ratio in measurements from a spherical neuron of 25 μm diameter as function of VSFP membrane density and maximum fluorescence response $\Delta F/F_0$ under conditions of vanishing background fluorescence (f_B= 0) and 5 kHz sampling. Values of S/N are color coded according to the scale in (D). S/N was calculated from Eq. S1.7 with parameters as given in the text (see Methods). **(D)** S/N ratio as function of sampling interval Δt and maximum response $\Delta F/F_0$ assuming 500 units/μm^2 of VSFP and vanishing background fluorescence (f_B= 0). **(E)** Same as (C) but assuming a fraction of unresponsive background fluorescence f_B of 80 %. **(F)** Same as (D) but assuming 80% background fluorescence.

Supplement 4
Overview of VSFP simulation models

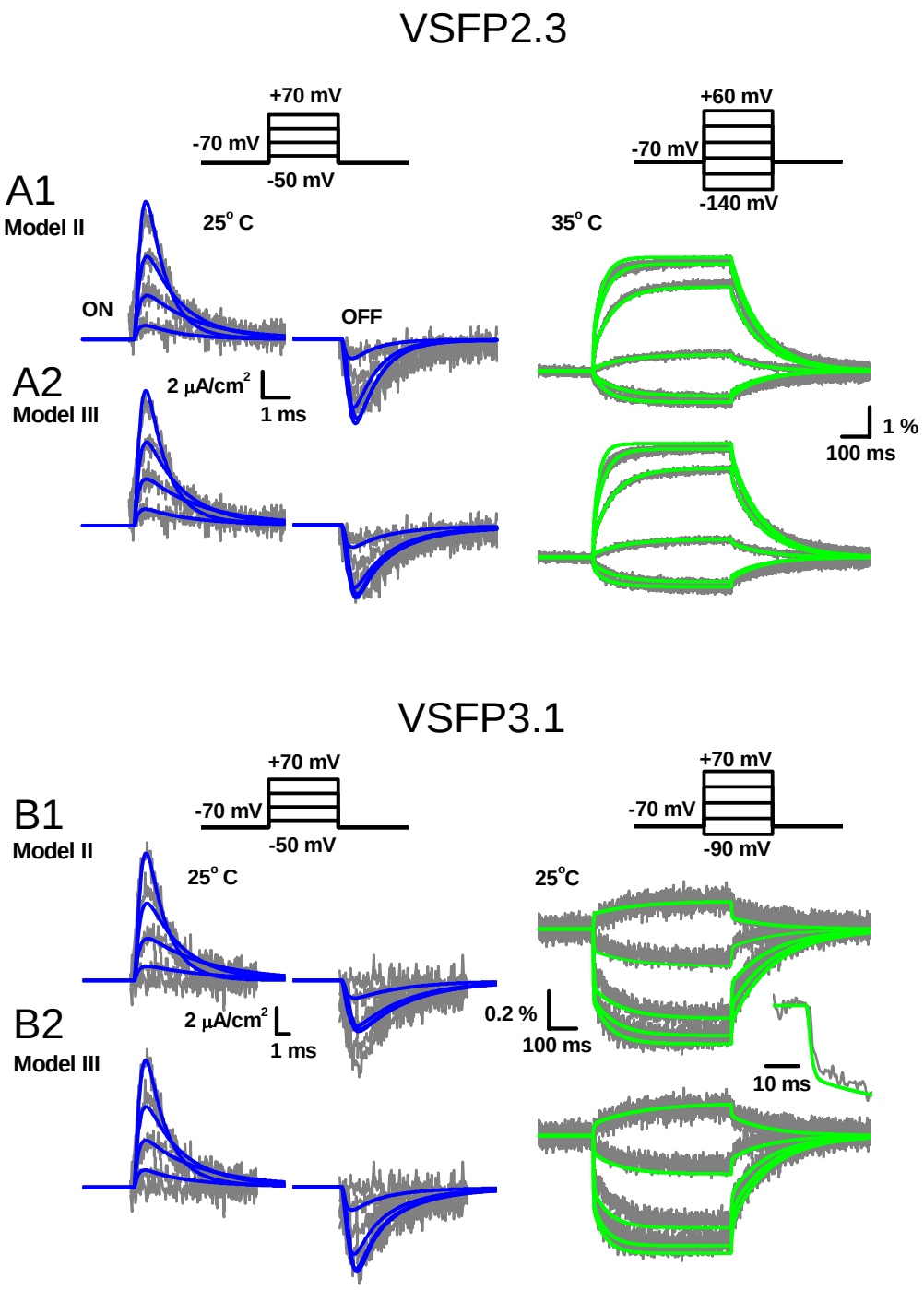

Fig. S2: Simulations of sensing currents and fluorescence responses of VSFP2.3 and VSFP3.1 are in agreement with experimental data of these proteins.
(A1) Family of simulated sensing currents (blue) and YFP fluorescence traces (green) using VSFP2.3 Model II are shown together with corresponding experimental traces (grey). The

applied voltage-clamp protocol consisted of 20 ms (sensing response) or 500 ms (fluorescence response) long steps with 40 mV increments from a holding potential of -70 mV as indicated on top of the figure. The experimental traces are identical to those displayed in Fig. 4. The temperature was set to 25º (sensing response) and 35º (fluorescence response) to match the conditions of the experiments (see legend to Fig. 4 and related text). **(A2)** Same as (A1), but simulations performed with Model III instead of Model II. **(B1)** Simulations (blue: sensing; green: fluorescence) and measured traces of sensing currents and fluorescence responses (grey) for VSFP3.1. The experimental traces were recorded from the same cells at 25º (see Methods) by applying the voltage step protocol shown on top with step durations of 20 and 500 ms as in (A1). The simulations were performed using VSFP3.1 Model II. **(B2)** Same as (B1), but simulations performed with VSFP3.1 Model III instead of Model II. The initial fast fluorescence response to +70 mV depolarization at extended time scale is shown as inset.

Supplement 5
Simulations of VSFP2.3 and VSFP3.1 capacitance effects in Purkinje and L5 pyramidal neurons

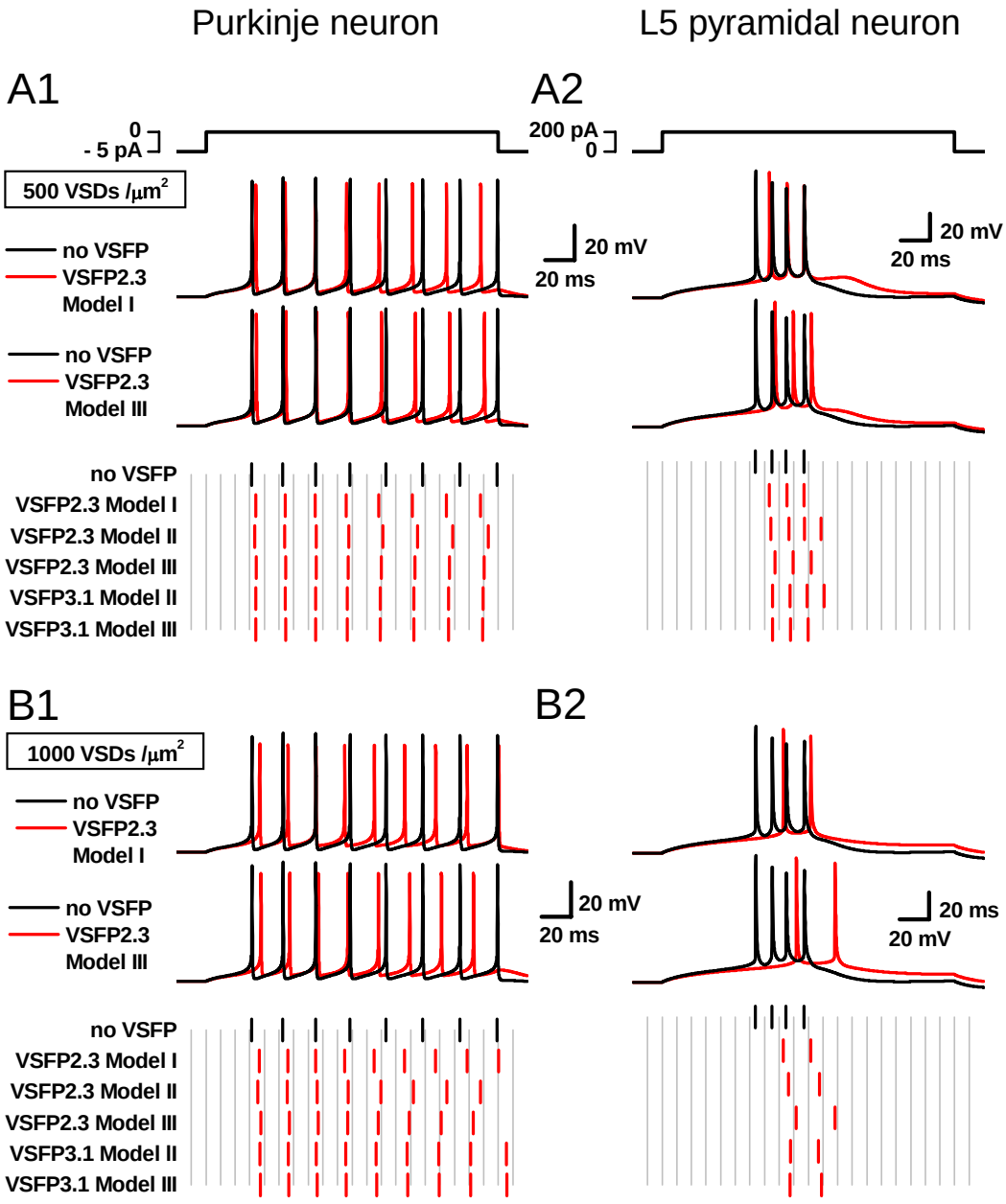

Fig. S3: Different computational models of VSFP proteins cause similar time shifts of evoked action potentials in simulated neurons.
(A1) Trains of action potentials in the Purkinje neuron model including VSFP with a surface density of 500 VSDs/µm^2 are evoked by current pulse injection (200 ms) into the cell body according to the protocol shown on top. The voltages traces show the evoked spike train in the presence of VSFP2.3 (top red trace: Model 1; lower red trace: Model III) in the membrane in comparison with the control case (no VSFP: black traces). Below shown are the

raster plots of action potential occurrence in the presence of VSFP (red bars) and control (no VSFP: black bars) for all models considered in this work. **(A2)** Same type of data as in (A1), but simulations performed using the L5 pyramidal neuron model. **(B1)** Same simulations as in (A1), but applying a capacitive load of 1000 VSDs/μm^2 compared to 500 VSDs/μm^2 in (A1). **(B2)** Same simulations as in (A2), but applying a capacitive load of 1000 VSDs/μm^2 compared to 500 VSDs/μm^2 in (A2).

Supplement 6
Effects of VSFP2.3 sensing capacitance on the spiking behavior of the Hodgkin-Huxley (HH)-model

To test for the effect of VSFP sensing capacitance in a simplified model, we examined the case of an excitable membrane containing two voltage gated ion channels: a Na^+ and a delayed rectifying K^+ channel, both described by classical Hodgkin-Huxley kinetics. The kinetic parameters were taken from the work of Wang et al. (Wang, X.J., Y. Liu, M.V. Sanchez-Vives, and D.A. McCormick. 2003. *J. Neurophysiol.* 89: 3279-3293) and are reproduced here for completeness.

The sodium current (Eq. 2 with X = Na, $m_{Na} = 3$) was $I_{Na} = G_{Na}\, n_{Na}^3\, h_{Na}\, (V\text{-}E_{Na})$ with the state variables n_{Na} and h_{Na} described by the following rate coefficients (see Eq. 1):

$$\alpha_{n,Na}(V) = -0.1ms^{-1} \cdot (V + 33mV) / \{\exp[-(V + 33mV)/10mV] - 1\}$$
$$\beta_{n,Na}(V) = 4ms^{-1} \cdot \exp[-(V + 58mV)/12mV]$$
$$\alpha_{h,Na}(V) = 0.07ms^{-1} \cdot \exp[-(V + 50mV)/10mV]$$
$$\beta_{h,Na}(V) = 1ms^{-1} / \{\exp[-(V + 20mV)/10mV] + 1\}$$

The potassium current (X = K, $m_K = 4$; no inactivation) was obtained as $I_K = G_K\, n_K^4\, (V\text{-}E_K)$ with the activation variable n_K given by the following rate coefficients:

$$\alpha_{n,K}(V) = -0.01ms^{-1} \cdot (V + 34mV) / \{\exp[-(V + 34mV)/10mV] - 1\}$$
$$\beta_{n,K}(V) = 0.125ms^{-1} \cdot \exp[-(V + 44mV)/25mV]$$

The channels were included into a single-compartment model (D = 20 μm) with membrane capacitance C_m (1μF/cm^2) and a leak current $I_{leak} = G_{leak}\, (V\text{-}E_{leak})$. The kinetic parameters were as follows (values in brackets): G_{Na} (45 mS/cm^2), E_{Na} (55 mV), G_K (18 mS/cm^2), E_K (-80 mV), G_{leak} (0.1 mS/cm^2), E_{leak} (-65 mV) and q_{10} (4).

Fig. S4 (see next page): VSFP2.3 sensing capacitance affects in a similar manner the timing of action potential spikes in two single-compartment cells containing different ion channel mechanisms.
(A) Simulation traces using a model cell containing voltage-gated Na^+ and K^+ channels with Hodgkin-Huxley (HH) kinetics. The panel shows (from top to bottom) the current step protocol for stimulating the cell, the membrane voltage, the Na^+ membrane current, the K^+ membrane current and VSFP sensing current for zero membrane expression (control; black traces) and with 1000 VSDs/μm^2 of VSFP2.3 (Model I; red traces). **(B)** Pullouts of overlaid traces in (A) covering the range of the second spike. The overlays were obtained by alignment to peaks of the voltage traces. **(C)** Pullouts of traces in (A) covering the range of the first three spikes at expanded y-scale as indicated in the figure. **(D-F)** Same as (A-C), but using the Purkinje neuron model (see Methods) instead of the HH-model.

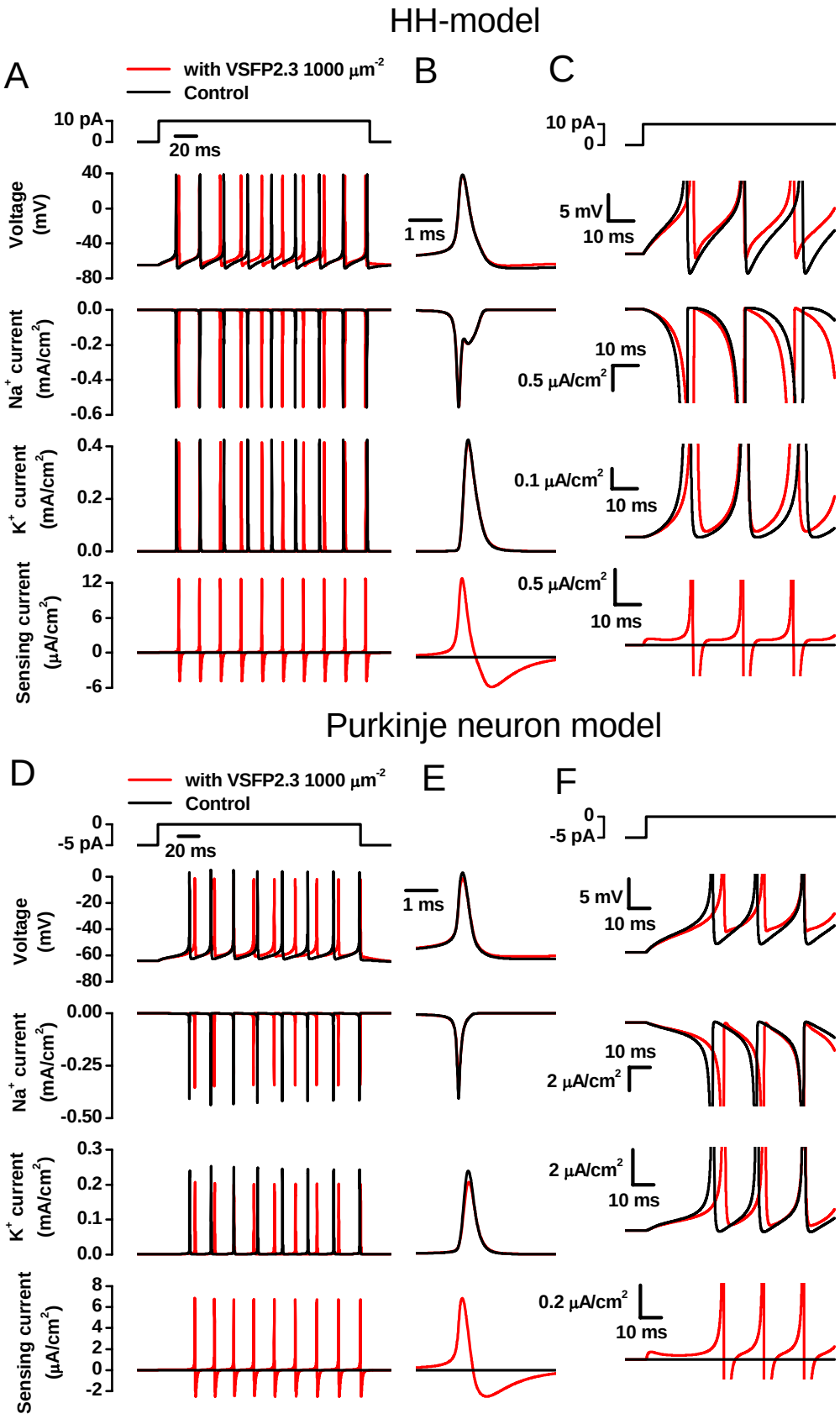
HH-model
A
B
C
with VSFP2.3 1000 μm-2
Control
10 pA
0
20 ms
Voltage (mV)
40
0
-40
-80
1 ms
5 mV
10 ms
Na+ current (mA/cm2)
0.0
-0.2
-0.4
-0.6
10 ms
0.5 μA/cm2
K+ current (mA/cm2)
0.4
0.2
0.0
0.1 μA/cm2
10 ms
Sensing current (μA/cm2)
12
6
0
-6
0.5 μA/cm2
10 ms
Purkinje neuron model
D
E
F
with VSFP2.3 1000 μm-2
Control
0
-5 pA
20 ms
Voltage (mV)
0
-20
-40
-60
-80
1 ms
5 mV
10 ms
Na+ current (mA/cm2)
0.00
-0.25
-0.50
10 ms
2 μA/cm2
K+ current (mA/cm2)
0.3
0.2
0.1
0.0
2 μA/cm2
10 ms
Sensing current (μA/cm2)
8
6
4
2
0
-2
0.2 μA/cm2
10 ms

Supplement 7
Effect of VSFP2.3 ON and OFF sensing current on spike trains in the Purkinje neuron model

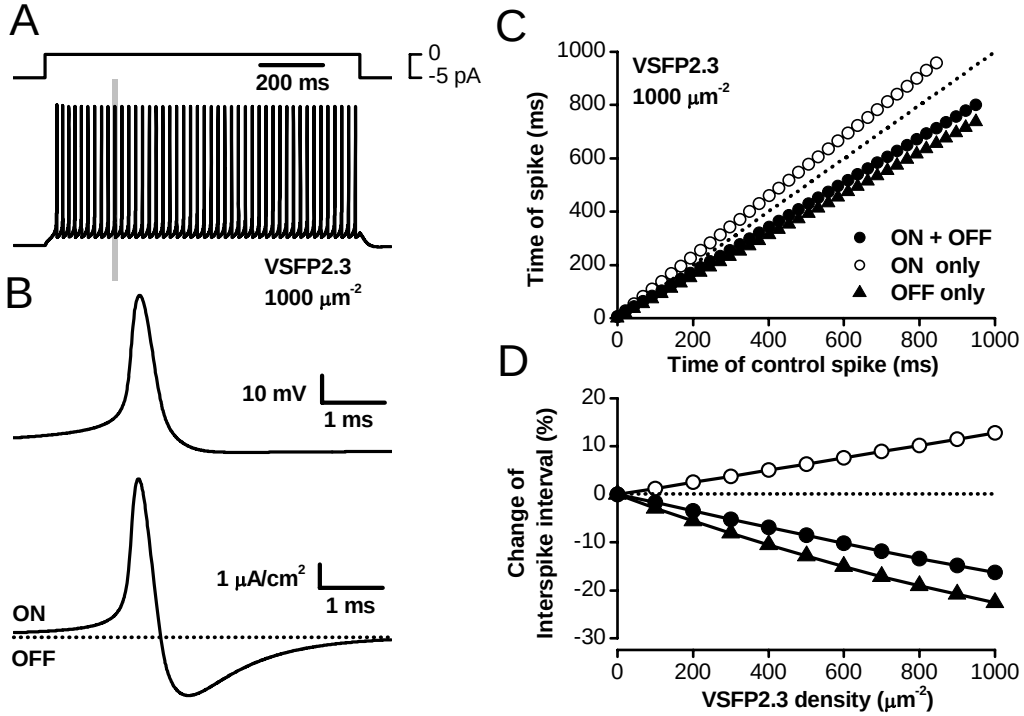

Fig. S5: VSFP expression-induced decrease of interspike periods in simulated Purkinje neuron spike trains.
(A) Train of spontaneous action potentials in the Purkinje neuron model, including 1000 units/μm^2 of VSFP2.3 (Model I), as elicited by the current stimulus shown on top. **(B)** Top panel: A single action potential (marked gray in (A)) at enlarged time scale (top panel) together with the VSFP2.3 sensing current (lower panel). Zero current is indicated as dashed line. **(C)** Times of spike events in the spike train shown in (A) versus spike events in the control case (VSFP2.3 not included) for the full VSFP2.3 kinetic model (ON + OFF; full circles), the same model with truncated OFF current (ON only; open circles) and with truncated ON current (OFF only; open triangles)**.** The dashed line corresponds to zero spike shift. **(D)** Change of interspike interval as function of VSFP2.3 membrane density produced by using the full and the truncated VSFP models (same as in (C)).

Supplement 8
Subcellular targeting of VSFPs can reduce physiological effects of VSFP sensing capacitance

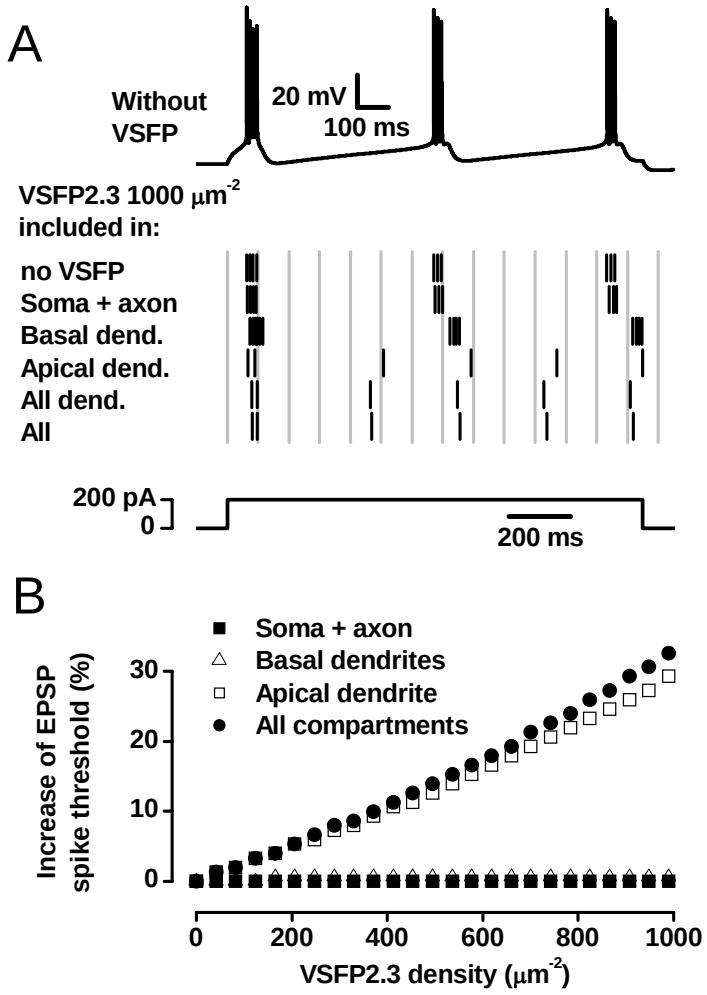

Fig. S6: Targeting of VSFP to subcellular compartments reduces capacitive effects in the L5 pyramidal neuron model.
(A) Somatic action potentials evoked by a current pulse of 200 pA injected into the cell body (bottom panel) for the control model (no VSFP included; top panel) and after including 1000 units/μm^2 of VSFP2.3 (Model I) in different compartments (middle panel: soma + axon; all 10 basal dendrites; all segments of the apical dendrite; all dendritic compartments; the whole cell). **(B)** Increase of threshold distal synaptic conductance (rise: 0.3 ms; decay: 3 ms) for somatic spike initiation (in per cent versus control) versus density of VSFP2.3 in different cellular compartments (soma + axon; the basal dendrites; the apical dendrite; the whole cell). EPSPs were elicited in the distal apical dendrite as described in the text.